Temp#42348
83N 23629

NASA Contractor Report 168225

A TOTAL LIFE PREDICTION MODEL FOR STRESS CONCENTRATION SITES

G. A. Hartman and D. S. Dawicke

University of Dayton
Dayton, Ohio

(NASA-CR-168225) A TOTAL LIFE PREDICTION MODEL FOR STRESS CONCENTRATION SITES Final Report (Dayton Univ., Ohio.) 33 p HC A03/MF A01 CSCL 20K

N84-10612

Unclas
G3/39 42348

September 1983

Prepared for

NATIONAL AERONAUTICS AND SPACE ADMINISTRATION
Lewis Research Center
Under Grant NAG 3-246

TABLE OF CONTENTS

SECTION 1
INTRODUCTION

The growth of cracks can be divided into the two categories of initiation and propagation. In a notched structure, the initiation and subsequently the propagation of small cracks are governed by the stress field created by the notch. After the crack grows beyond the influence of the notch, crack propagation is controlled by the nominal stress in the structure.

In the current study we have divided the total life prediction problem into three tasks. These tasks are:

- Determine the crack length where the initiation phase terminates and the propagation phase begins.
- Provide an estimate of the number of cycles to initiate a crack.
- Provide an estimate of the number of cycles to propagate the crack to failure.

Relative proportions of initiation and propagation lives are dependent on the crack length chosen to delineate the two regimes. Dowling [1] has proposed a method of estimating the appropriate crack length by comparing a short crack stress intensity with a long crack stress intensity. Modification of this model may be necessary to account for compressive residual stress generated during first cycle yielding for positive load ratios.

The most promising method for estimating initiation life is based on notch strain amplitude. Calculations of notch strain based either on a Neuber analysis or finite element results are used in conjunction with strain-life data to generate life estimates for the initiation of a crack. Care must be taken to properly define failure when generating the strain-life data. The definition of failure must coincide with the model used to estimate the crack length delineating initiation and propagation.

The linear elastic parameter-K was chosen to correlate fatigue crack growth rate data and to make life predictions for the propagation phase of the specimen life. Corrections were included for both finite width and corner crack geometries. The K-parameter was chosen because of its simplicity and established methodology. Based on recent studies by Leis et al. [2] and El Haddad et al. [3], it was anticipated that anomalous small crack behavior would be observed causing K to be inappropriate for fatigue crack growth rate correlations and life predictions. The anomalous behavior was not observed in any of the tests and sophisticated methods which address this problem are not warranted in this study.

SECTION 2
MATERIAL AND TESTING PROCEDURES

A description of the material and experimental procedures is presented in this section. A test condition summary and a description of sample geometries are also included.

2.1 MATERIAL AND TEST CONDITIONS

2024-T3 aluminum was chosen as a representative airframe alloy. Some crack growth data are already available in the literature [4] for this material which will be used for comparison to data generated during this project. Tensile material characterization tests have been completed and tensile test data is shown in Figure 1 for two replicate tests. Cyclic stress-strain data and strain-life data are currently being generated.

A summary of tests conducted to date is presented in Table 1. Figure 2 shows the specimen geometries used in the various tests.

2.2 EXPERIMENTAL PROCEDURES

All tests were performed on an MTS servohydraulic test system. Loads were measured with a calibrated load cell placed in series with the sample. Strains were measured with an axial extensometer with a 0.5 inch gage length. Cycle counts were recorded from a mechanical counter. Crack lengths were measured with traveling microscopes with a magnification of 20x. These units can resolve crack lengths on the order of 0.0005".

All critical areas of the samples were machined and/or polished to a surface finish of 16 microns or less.

Some of the radially cracked holes (RCH) samples were intentionally scratched on one side of the hole to guarantee growth on one side only. These tests were used to generate crack propagation data only and are labeled in Table 1.

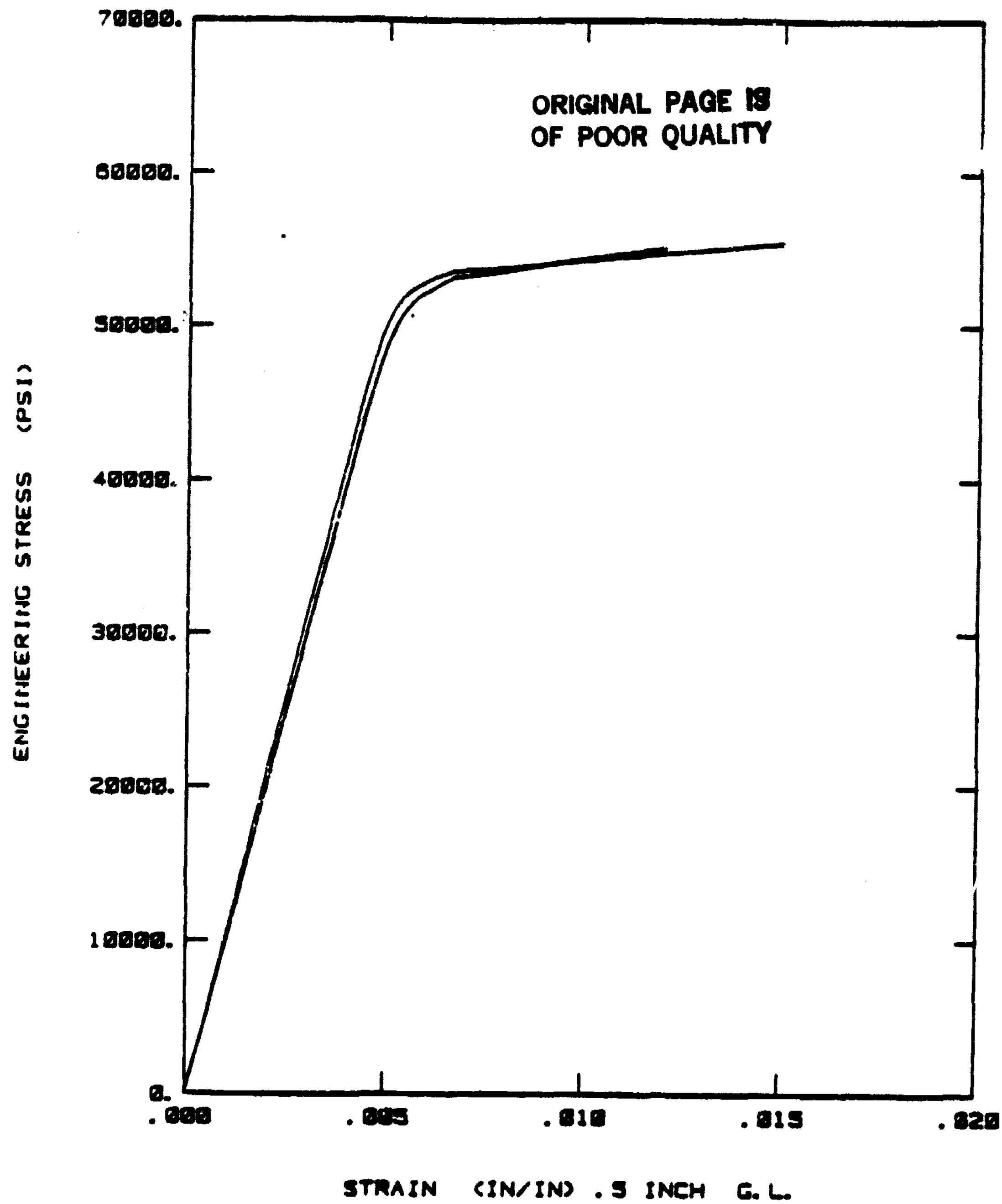

Figure 1. Tensile Properties for 2024-T3 Aluminum T=75^{o}F, $\dot{\varepsilon}$ = 0.001 in/in/sec - 2 Replicate Tests.

TABLE 1

TEST CONDITION SUMMARY

SPECIMEN ID	TEST TYPE	MAX LOAD (KIPS)	LOAD RATIO	THICKNESS (INCH)	WIDTH (INCH)
RCH1	Propagation	4.0	-1.0	0.1875	2.0
RCH2	Propagation	5.2	0.0		
RCH3		10.0	0.0		
RCH4		10.0	0.0		
RCH5		10.0	0.0		
RCH6		8.0	0.0		
RCH7	Propagation	8.0	0.0		
RCH8	Initiation & Propagation	10.0	0.0		
RCH9		10.0	0.0		
RCH10		5.5	-1.0		
RCH11		8.0	0.0		
RCH12	Intiation & Propagation	4.0	-1.0		
CCP1	Propagation	5.0	0.0		2.0
CCP2		6.0	0.0		4.0
CCP3		17.0	0.0		4.0
CCP4		5.5	-1.0		2.0
CCP5	Propagation	3.0	-1.0	0.1875	2.0

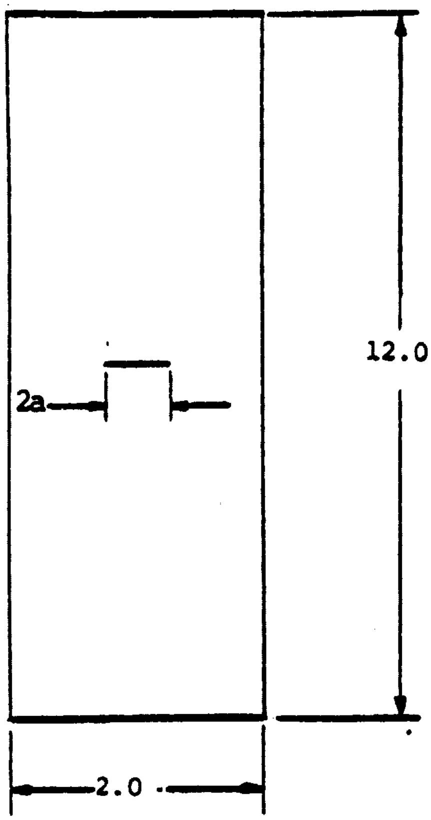

a) CCP geometry

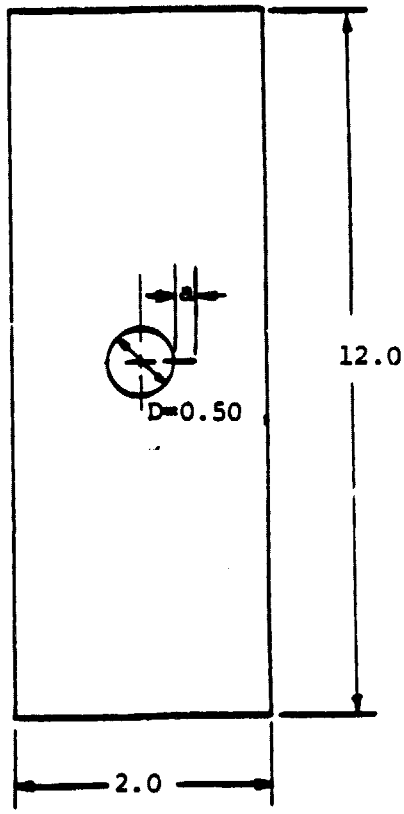

b) RCH geometry

NOTE: All Dimensions in Inches

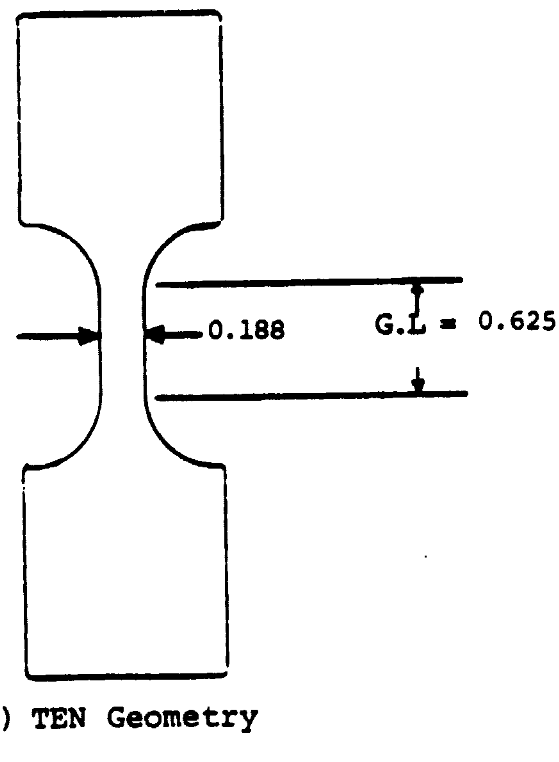

c) TEN Geometry

Figure 2. Specimen Geometries Used in This Study.

SECTION 3

LIFE PREDICTION MODELS

Two life prediction models were chosen for additional study. These include one initiation model and one propagation model.

3.1 STRAIN-LIFE INITIATION MODEL

The chosen initiation model is based upon the idea that equal strain amplitudes and mean stresses in two structures will give equal crack initiation lives. Use of this model requires some knowledge of notch stress-strain behavior. To gain an understanding of the possible strain amplitude and mean stress conditions at the notch root of an uncracked RCH sample, it is necessary to analyse the loading conditions that a sample will see.

Figure 3 illustrates the possible notch root stress-strain responses under various levels of applied stress. For the highest loads, the notch root may experience both tensile and compressive yielding on each cycle regardless of load ratio because inelastic action at the notch tends to eliminate any mean stress effects. This behavior is illustrated in Figure 3a. The strain amplitude can be obtained through a Neuber or finite element analysis and the mean stress is zero. The lower bound on this regime can be estimated by noting that the notch root material will exhibit linear elastic behavior on unloading and that K_t is still valid unless gross specimen deformation has occurred.

$$K_t \, \Delta S_{Limit} = 2\sigma_Y$$
$$\Delta S_{Limit} = \frac{2\sigma_Y}{K_t} \qquad (3.1)$$

where

ΔS_{Limit} = lower limit of applied stress range for reversed yielding

σ_Y = yield strength

K_t = elastic stress concentration factor

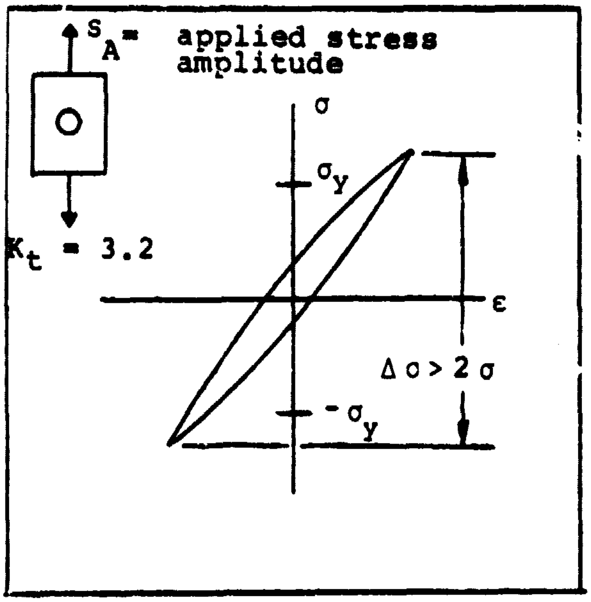

a) $S_A * K_t > \sigma_{yield}$. Notch root stress ratio tends toward zero regardless of applied stress ratio.

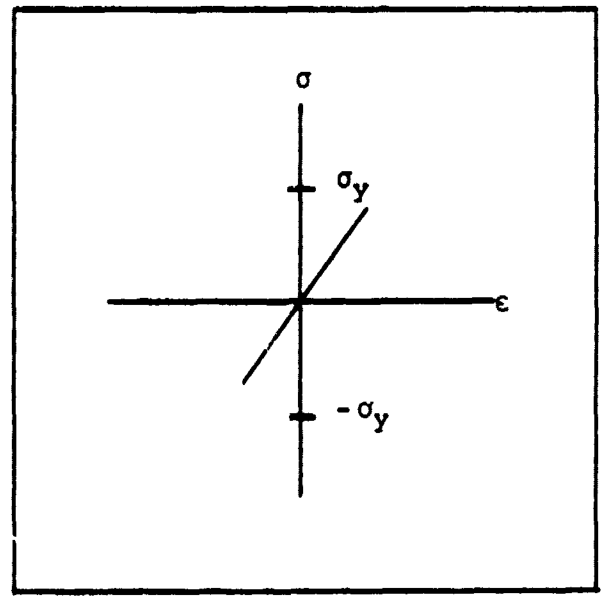

b) $S_A * K_t \leq \sigma_{yield}$ and $R_{applied} = -1$.

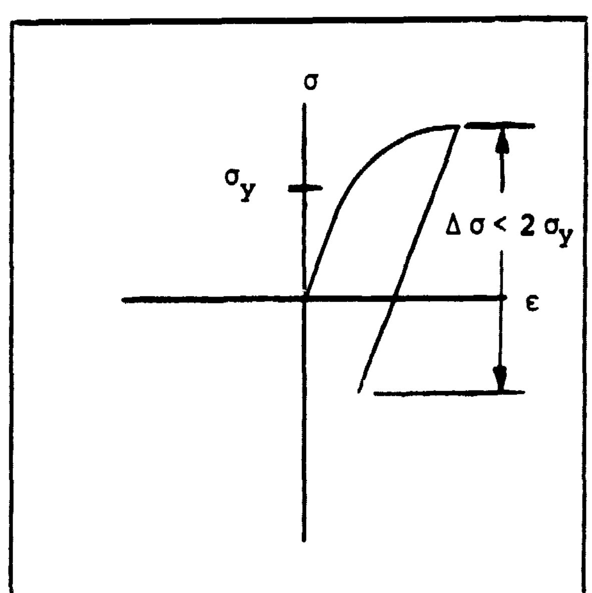

C) $S_A * K_t > \sigma_y$ but $R_{applied} > -1$ so yielding can take place on first cycle. This situation generates residual stresses.

Figure 3. RCH Sample Notch Root Response for Various Applied Stress Amplitudes and Stress Ratios.

For applied stress ranges lower than ΔS_{Limit}, the cyclic stress excursions are elastic. Let us now limit ourselves to applied stresses lower than ΔS_{Limit}.

For fully reversed loading (R=-1) the notch root will cycle elastically between $+K_t \Delta S/2$ and $-K_t \Delta S/2$ (Figure 3b). For load ratios greater than -1 two possibilities exist. First, if $K_t S_{max} < \sigma_y$ (where S_{max} is the maximum applied stress) then the notch exhibits elastic behavior with a mean stress equal to $K_t (S_{max} + S_{min})/2$. If however $K_t S_{max} > \sigma_y$ than the notch root will yield on the first cycle. Recall that the stress range is limited by $\Delta S < 2 \sigma_y/K_t$. Under these conditions, the notch root material will unload elastically and subsequent cycles will cause elastic response with a tensile mean stress as shown in Figure 3c.

These descriptions of notch root behavior allow us to predict the strain amplitude and mean stress experienced at the notch for a variety of loading conditions. The predicted mean stress and strain amplitude can be used in conjunction with a strain-life diagram and a mean stress model to obtain an estimate of the number of cycles to initiate a crack of predetermined length.

Tests are currently being conducted to generate strain-life data for the 2024-T3 alloy. Care is being taken to record initial cracking, intermediate stages of cracking, and final separation of the sample to allow various definitions of smooth specimen failure to be identified. In order to exercise the model, 2024-T351 data will be used from the literature [4] until material characterization tests can be completed.

In order to predict the mean stress effects, a model presented by Sandor [5] was chosen for study.

ORIGINAL PAGE IS
OF POOR QUALITY

$$2N_f = \left(\frac{\sigma_a}{\sigma_f' - \sigma_m} \right)^{1/b} \tag{3.2}$$

where

N_f = cycles to failure

σ_a = applied stress amplitude

σ_f' = fracture strength coefficient

σ_m = mean stress

This model was chosen for its simplicity and ability to correlate strain life data. Modifications will be made as required.

3.2 INITIATION CRACK LENGTH ESTIMATION MODELS

To determine the proper crack length for use in delineating initiation and propagation of a crack we have chosen a method proposed by Dowling [1]. This method is based on comparison of elastic stress-intensity solutions for short cracks growing at a notch and traditional long cracks. The initiation crack length is defined as ℓ_m, the intersection of the short and long crack stress-intensity factors.

$$\ell_m = \frac{r}{(1.12K_t)^2 - 1} \tag{3.3}$$

It should be noted that this model is based on elasticity and does not include residual stress effects.

Residual stresses will be present at the notch when monotonic inelastic action is followed by cyclic elasticity. The size of the zone in which residual stresses are present can be estimated from finite element techniques. Figure 4 illustrates three possible combinations of ℓ_m and residual stresses. If the initiation crack length is chosen much smaller than the zone of residual stress (ℓ_{m1}), then the residual stresses will be active throughout the initiation phase and a straightforward correction can be made using the mean stress model in Subsection 3.1. If the initiation crack length is chosen approximately equal to the residual stress zone, (ℓ_{m2}), then the residual stress at an initiating crack tip will fall off as the crack grows to length ℓ_m. In this case, some "average" mean stress

ORIGINAL PAGE IS
OF POOR QUALITY

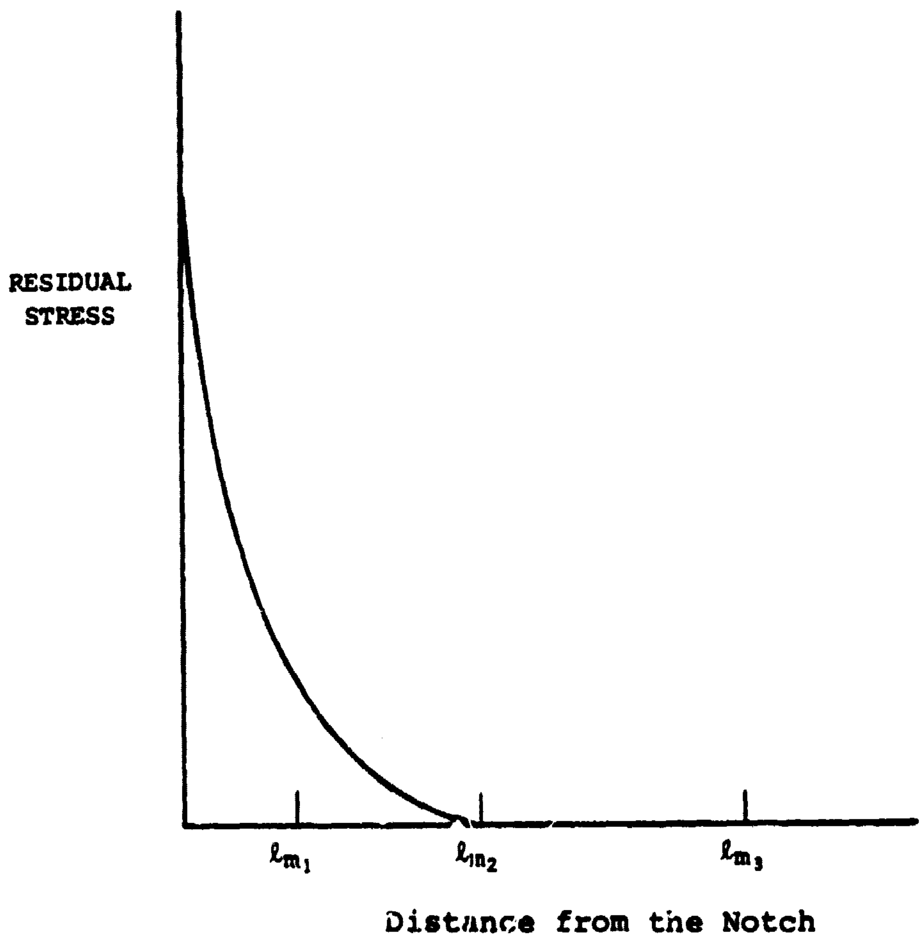

Figure 4. Residual Stress at Notch and Three Initiation Crack Lengths.

correction will be necessary. If the residual stress zone is much smaller than the chosen initiation crack length (ℓ_{ms}), then the residual stresses will be active only during the beginning of the initiation phase. In this case, it may be necessary to breakup the initiation phase into residual stress dependent and residual stress independent sections.

3.3 ELASTIC PROPAGATION MODEL

The Linear Elastic Fracture Mechanics parameter K, the stress-intensity factor, was chosen to predict crack propagation. For the CCP geometry, the secant method was used to account for the finite width of the specimen

$$K_{max} = \sigma_{max} \sqrt{\pi a \sec(\frac{\pi a}{w})} \qquad (3.4)$$

where

a = half crack length

σ_{max} = maximum applied stress

w = width of specimen

An empirical relationship between crack growth rate and stress-intensity factor can be determined from crack growth tests of standard geometries, such as a center crack panel.

$$\frac{da}{dN} = F\ (K) \qquad (3.5)$$

where

$\frac{da}{dN}$ = crack growth rate

F = empirical function

The RCH propagation life is defined as the number of cycles necessary to grow a crack from the initial crack length ℓ_m to a final crack length. Propagation life for the RCH samples can be estimated by integrating the empirical relationship F with respect to dN and da.

$$N_p = \int_{a_i}^{a_f} \frac{1}{F(k)}\, da \qquad (3.6)$$

where

N_p = propagation cycles

a_i = initial crack length = ℓ_m

a_f = final crack length

A closed form solution generally does not exist for the function F; thus, a numerical integration method must be employed to solve for the propagation life.

SECTION 4
EXPERIMENTAL RESULTS

The procedures and models described in the previous section were used to predict total lives of four RCH tests and the propagation model was used to predict propagation life for 12 RCH tests. The results of these predictions are presented in this section along with a discussion of the results. In addition, fatigue crack growth rate data were correlated with the elastic parameter K. The results and a discussion of these are also presented.

4.1 FATIGUE CRACK GROWTH RATE CORRELATIONS

Fatigue Crack Growth Rate (FCGR) data from all tests reported in Table 1 were correlated using the elastic stress-intensity factor. Two types of geometries were tested: center-crack panel (CCP) and radially cracked hole (RCH).

Figure 5 contains the FCGR data from the CCP tests with a load ratio of zero. A mean trend for these tests was obtained through an engineering estimate of the data. This mean trend consists of three linear segments on the logarithmic scale as shown in Figure 6. Also included in Figure 6 is additional FCGR data for 2024-T3 [6]. The mean trend of the FCGR data from this program agrees with the previous published data for 2024-T3.

Two additional CCP specimens were tested at a load ratio of -1.0, the results of these tests are presented in Figure 7 along with the mean trend of the data. The data was correlated in terms of K_{max} and compressive loading apparently does not affect the crack growth rate for this material and geometry as illustrated by the comparisons of the mean trends shown in Figure 8.

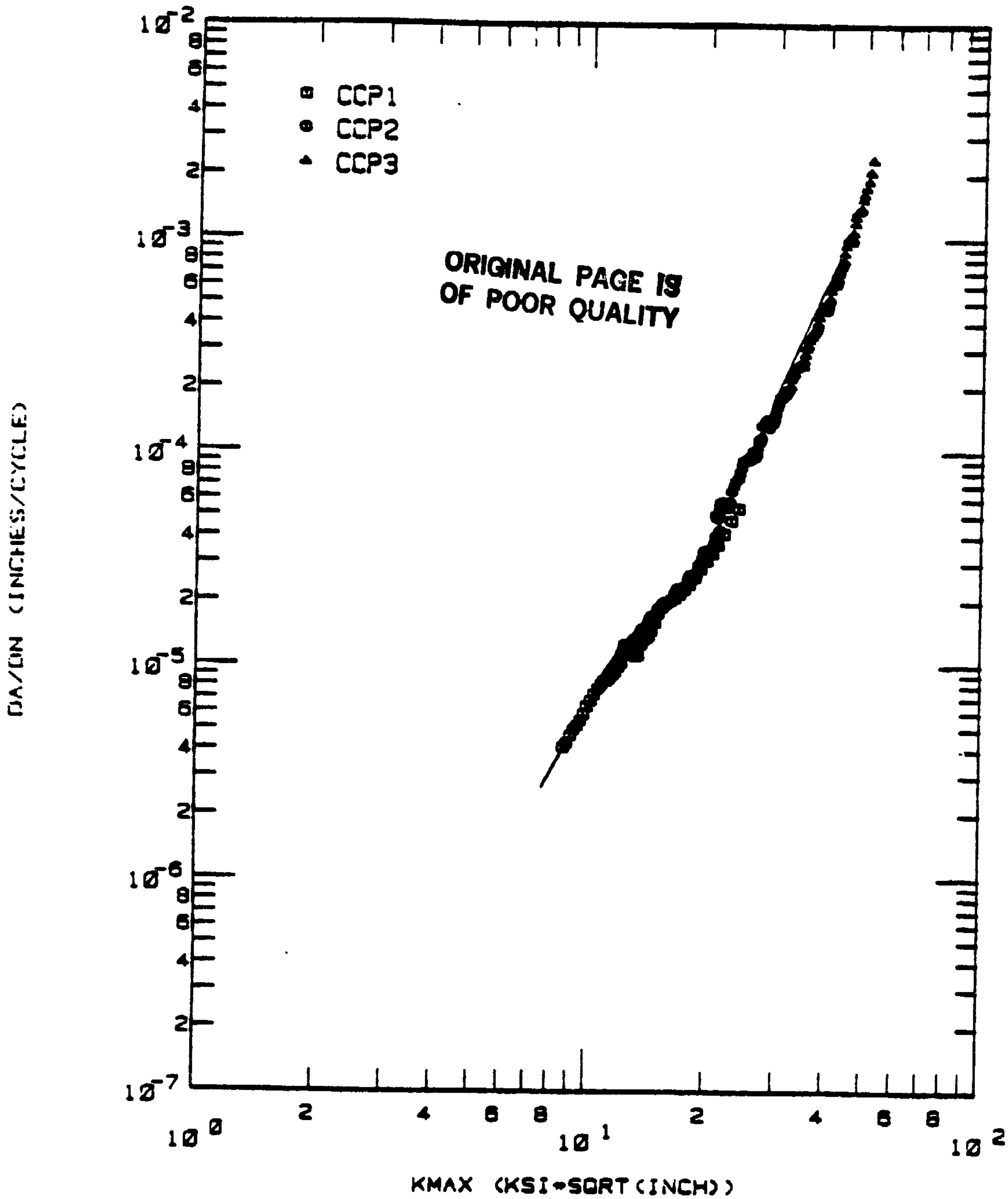

Figure 5. Fatigue Crack Growth Rate Data for Center-Crack Panel Specimens with a Load Ratio of 0.0 and Mean Trend Fit.

ORIGINAL PAGE IS
OF POOR QUALITY

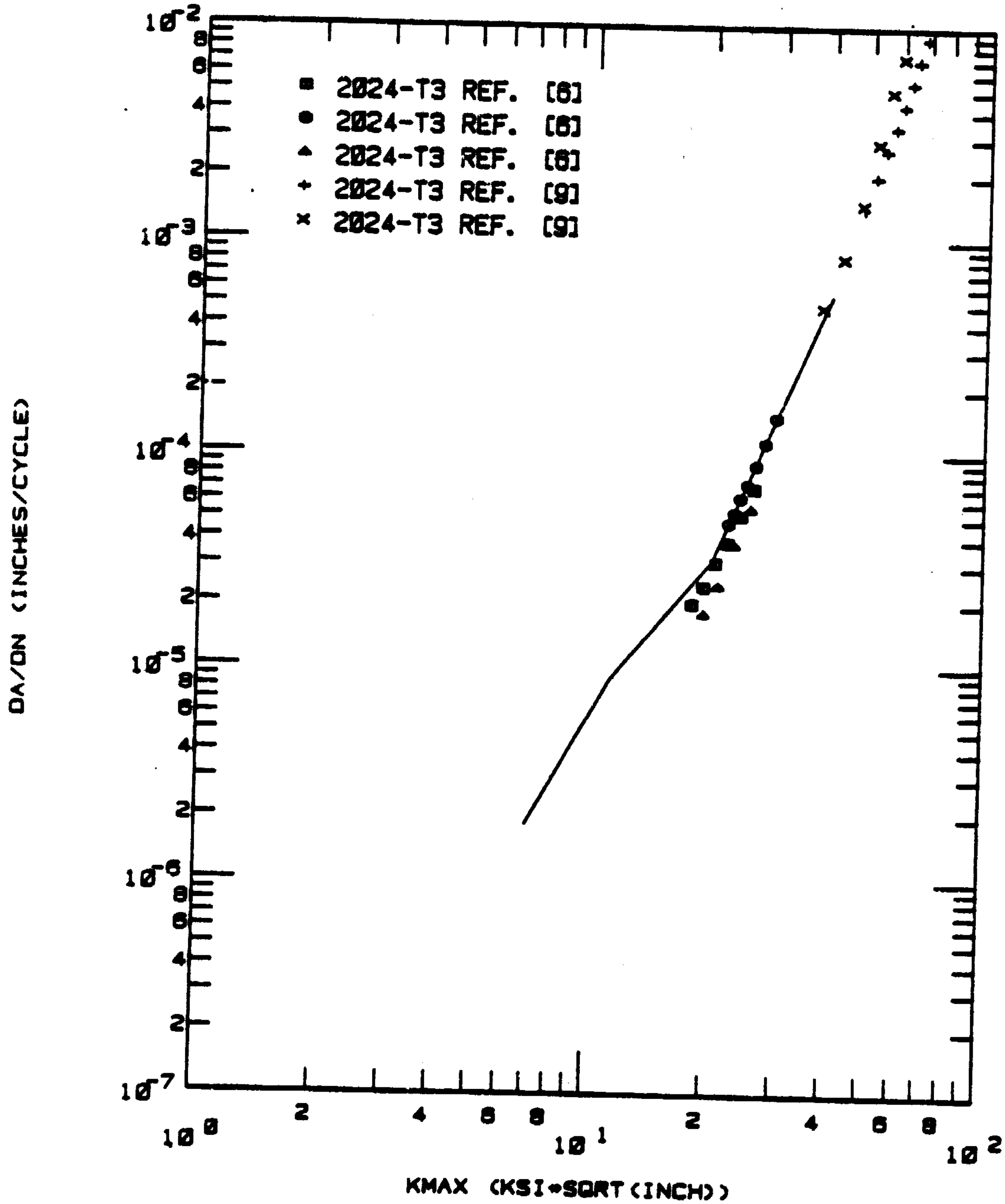

Figure 6. Mean Trend of Center-Crack Panel FCGR data from This Program and Previously Published Data for 2024-T3 [9]. Load Ratio = 0.0.

For the RCH tests, both through the thickness cracks and corner cracks were observed, as indicated in Table 2. The stress-intensity factor for the through-the-thickness crack was expressed as the least squares fit to the finite element results.

$$K_{max} = \frac{\sigma_{max}}{\sqrt{2}}[0.1164+30.99(\tfrac{a}{2})-164.8(\tfrac{a}{2})^2+458.7(\tfrac{a}{2})^3=619.4(\tfrac{a}{2})^4 +(329.9(\tfrac{a}{2})^5] \quad (4.1)$$

The stress-intensity factor for the corner crack was obtained from a solution developed by Newman and Raju [7,8]. A least squares fit was used to express the corner crack solution in a mathematical form.

$$K_{max} = \sigma_{max}[0.006695+10.8a+83.42a^2-1134a^3+3779a^4-3005a^5]^{\frac{1}{2}} \quad (4.2)$$

Figure 9 contains the corner crack and through-the-thickness crack stress-intensity factors.

The RCH tests were correlated using the two stress-intensity factor solutions as shown in Figures 10 and 11 for load ratios of 0.0 and -1.0 respectively. Also included in Figures 9 and 10 is the mean trend of the CCP FCGR data.

Table 2 contains the type of crack and smallest recorded crack length for the 12 RCH tests. The smallest crack size ranges from 0.001 inch to 0.035 inch, yet no anomalous nonconservative behavior associated with small cracks was observed. A decrease from the crack growth rate measured in the CCP tests was observed for the lowest K_{max} values of the RCH tests. This decrease may be caused by residual compressive stresses at the notch root. Additional work is planned to verify this hypothesis. The mean trends for the CCP tests at load ratios of 0.0 and -1 were used as the empirical function F(K) from Equation 3.4 in the life predictions of the RCH tests.

ORIGINAL PAGE IS
OF POOR QUALITY

TABLE 2

SUMMARY OF RCH FCGR TESTS

SPECIMEN ID	APPLIED STRESS (KSI)	LOAD RATIO	TYPE OF CRACK	SMALLEST RECORDED CRACK LENGTH (IN)
RCH1	10.67	-1.0	Corner	0.003
RCH2	13.87	0.0	Corner	0.013
RCH3	26.67	0.0	Corner	0.035
RCH4	26.67	0.0	Corner	0.005
RCH5	26.67	0.0	Through	0.003
RCH6	21.33	0.0	Through	0.009
RCH7	21.33	0.0	Through	0.007
RCH8	26.67	0.0	Through	0.010
RCH9	26.67	0.0	Through	0.001
RCH10	14.67	-1.0	Corner	0.010
RCH11	21.33	0.0	Corner	0.006
RCH12	10.67	-1.0	Corner	0.010

ORIGINAL PAGE IS
OF POOR QUALITY

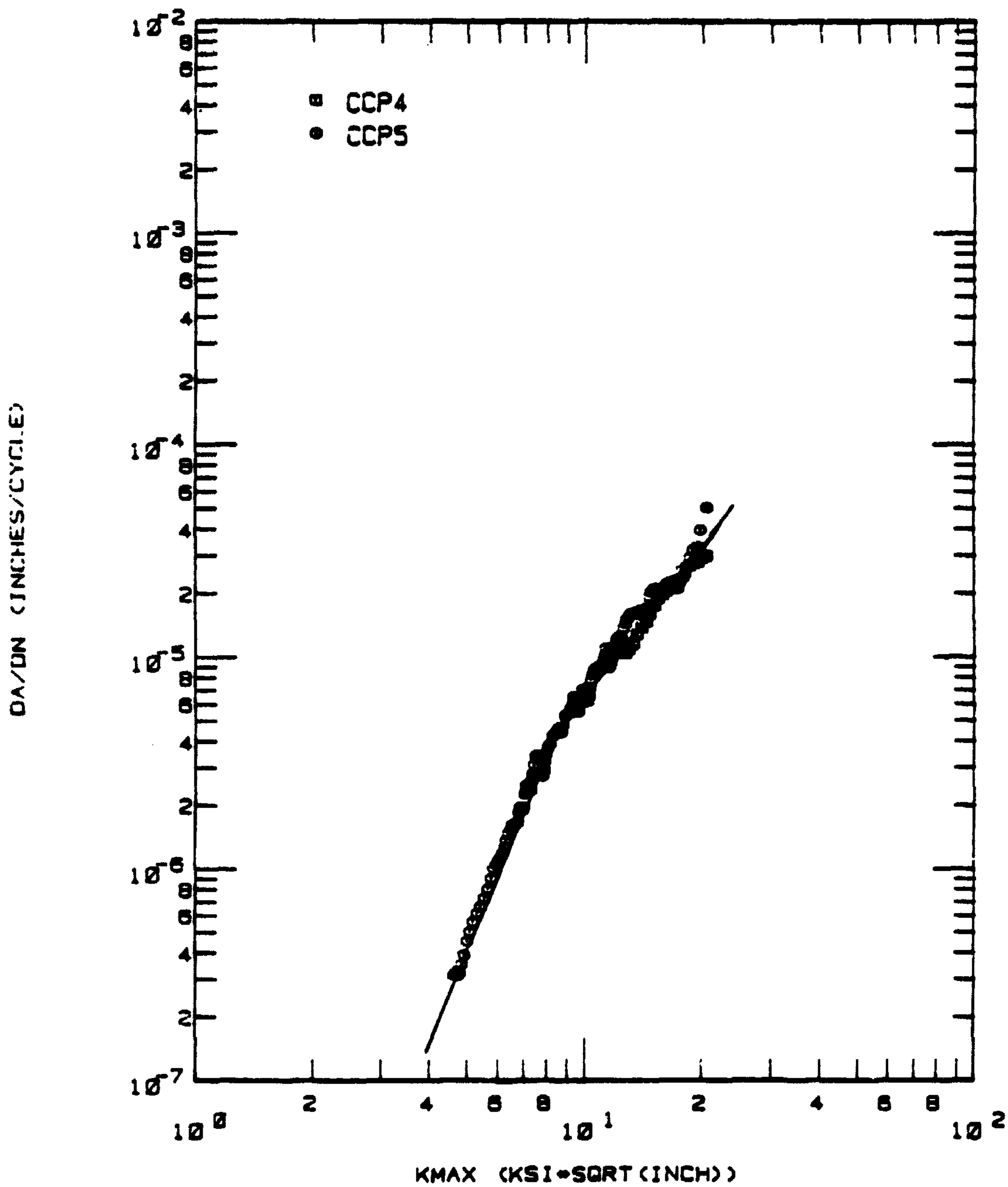

Figure 7. Fatigue Crack Growth Rate Data for Center-Crack Panel Specimens with a Load Ratio of -1.0, and Mean Trend Fit.

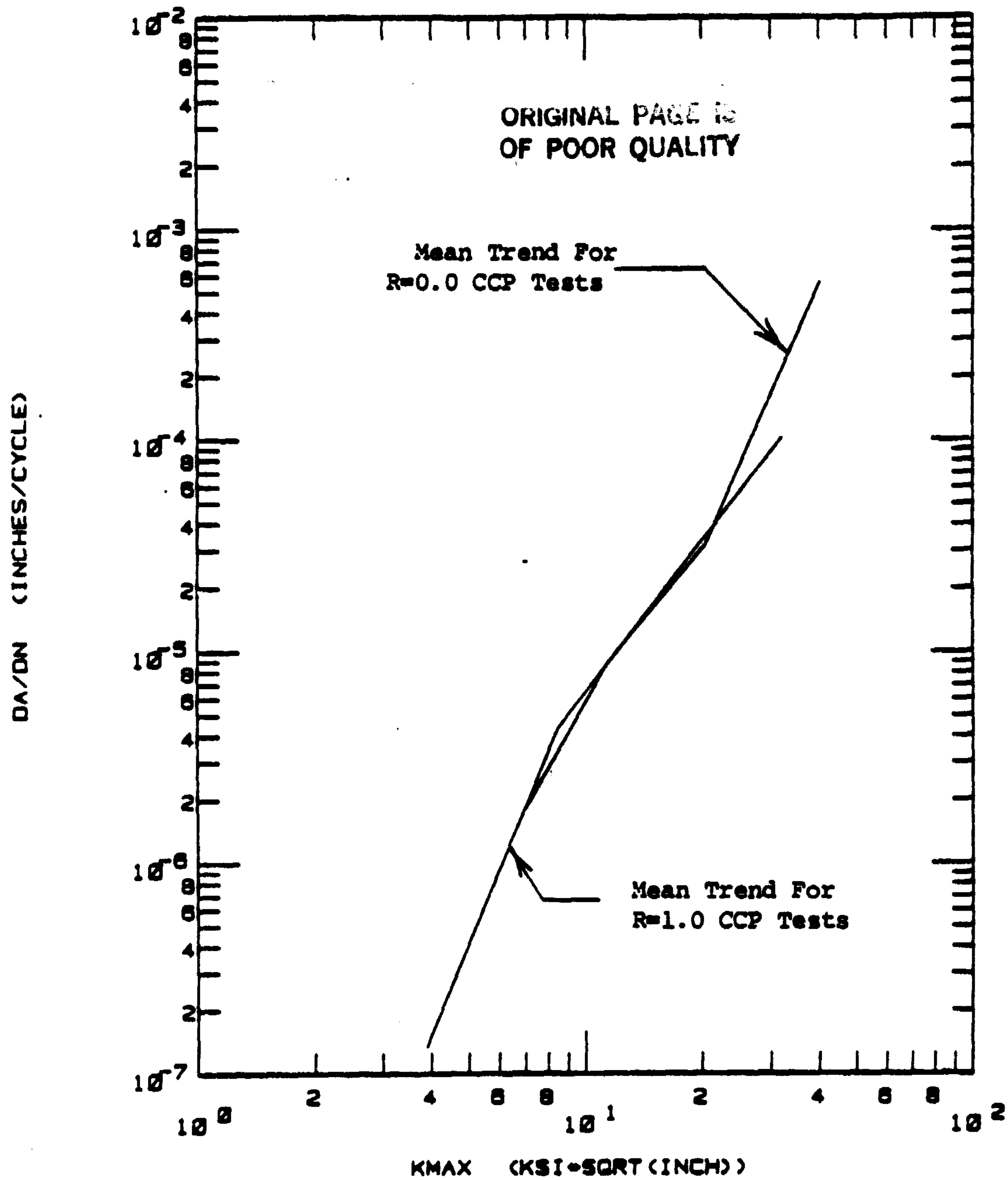

Figure 8. Comparison of Mean Trends for the CCP Tests at Stress Ratios of 0.0, and -1.0.

ORIGINAL PAGE IS
OF POOR QUALITY

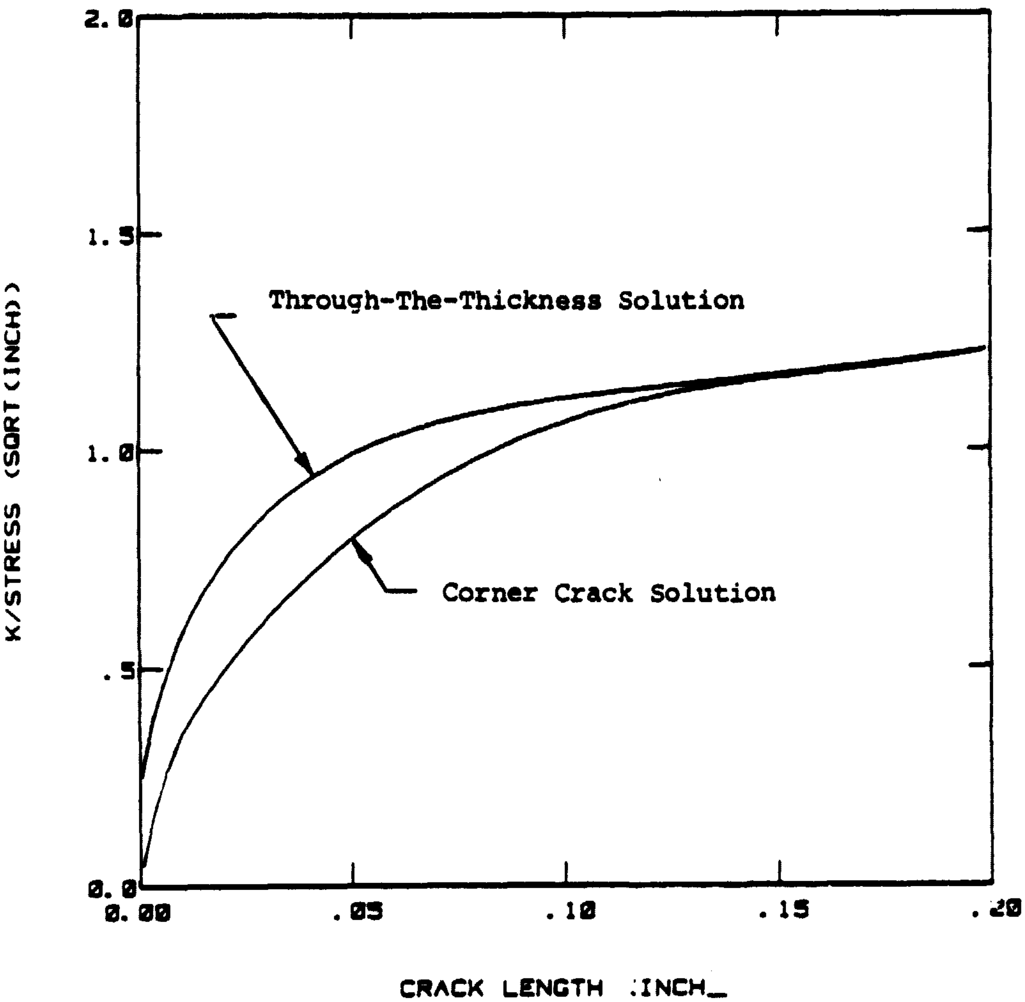

Figure 9. Elastic Stress-Intensity Factors for a Radial Cracked Hole Geometry.

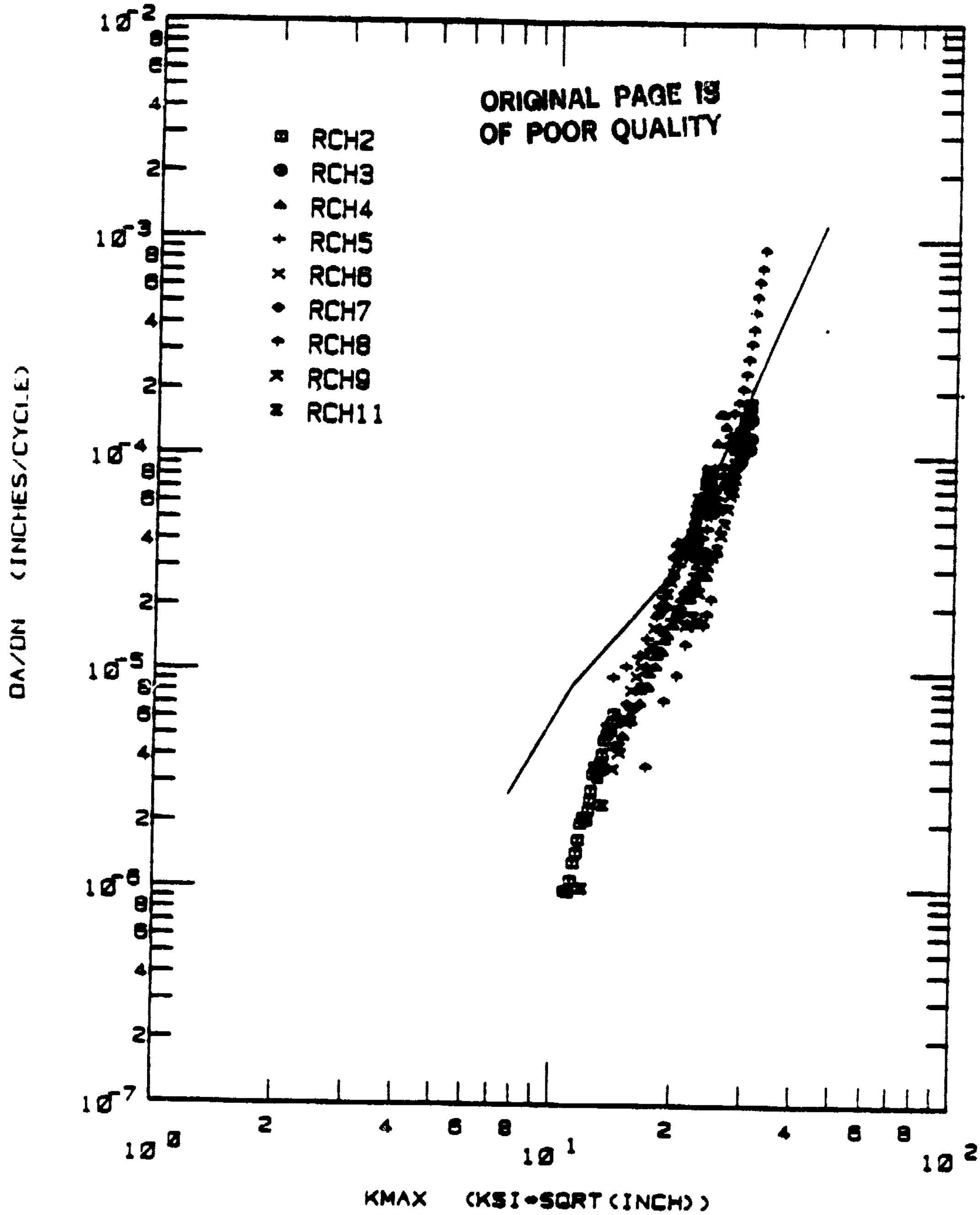

Figure 10. Fatigue Crack Growth Rate Data for the RCH Tests and the Mean Trend for the CCP Data, Load Ratio of 0.0.

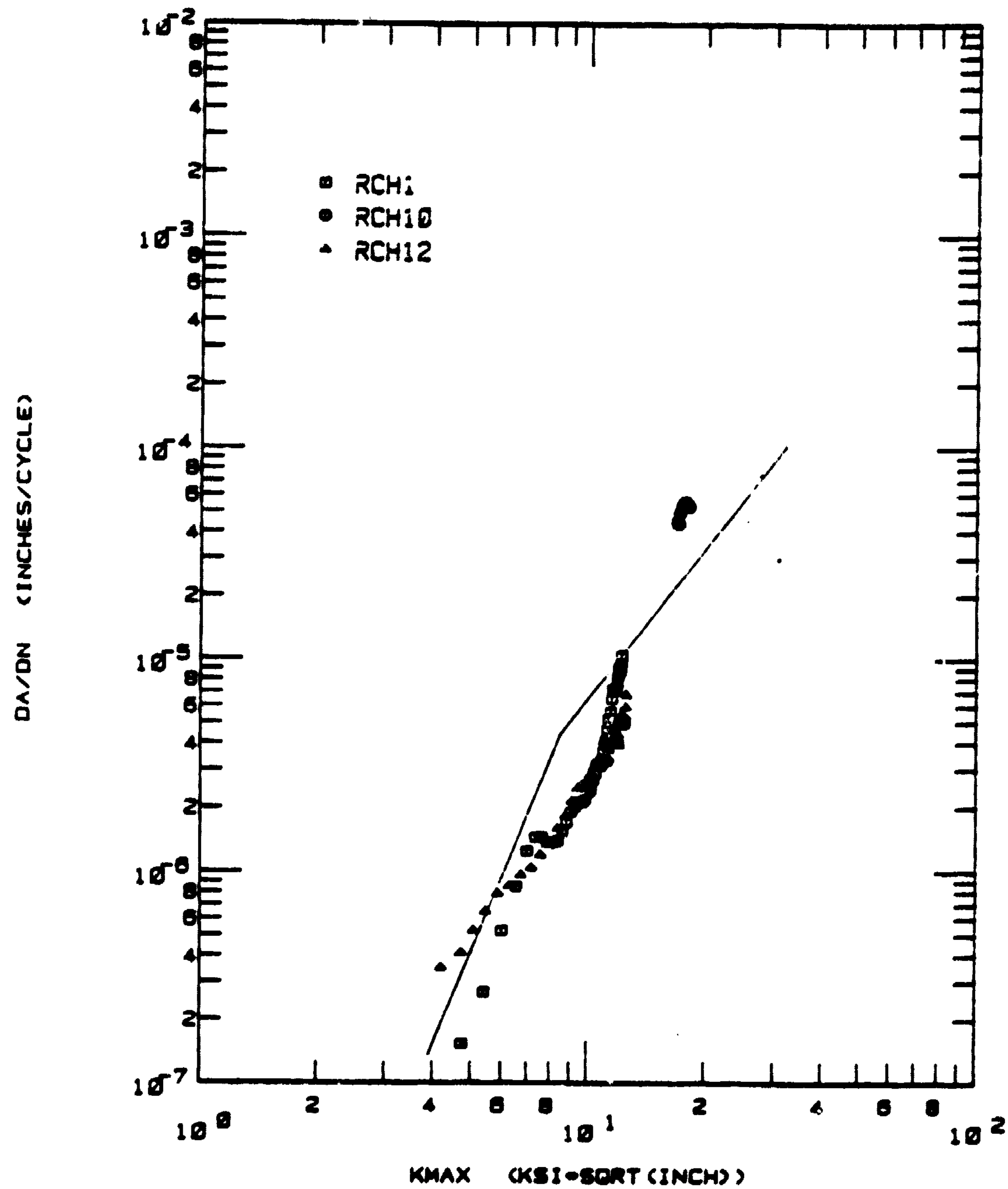

Figure 11. Fatigue Crack Growth Rate Data for the RCH Tests and the Mean Trend for the CCP Data, Load Ratio of -1.0.

4.2 INITIATION PREDICTIONS

Initiation life predictions were made for five RCH specimens as shown in Table 3. For sample RCH11, the maximum notch stress calculated from linear elasticity was 68.2 Ksi. The yield strength value was 54.0 Ksi; therefore, notch yielding had occurred. A Neuber analysis was used to determine that the actual notch stress was 54.5 Ksi. The minimum notch stress was the maximum notch stress minus the stress amplitude. For RCH11: minimum stress = 54.5 - K_t ΔS = 54.5 - 68.2 = -13.7 Ksi and the stress ratio becomes

$$R = \frac{-13.7}{54.5} = 0.25 \qquad (4.3)$$

rather than R=0.0 for the applied load.

The initiation predictions were calculated as outlined in Section 3.1. The ratio of predicted to actual life ranged from 0.253 to 0.957 for the five RCH specimens making all initiation predictions conservative. The results from specimen RCH9 are invalid due to a surface defect applied prior to the test.

4.3 PROPAGATION PREDICTIONS

Propagation life predictions were made for the 12 RCH specimens. The initial crack length ℓ_m was 0.023 inch and the final crack length was chosen to be 0.125 inch in each case. Unacceptable bending stresses were induced in the RCH specimens for crack lengths greater than 0.125 inch. These predictions are presented in Table 4.

The ratio of predicted cycles to actual cycles ranged from 0.26 to 0.988. Note that cracks which developed as through cracks had an average ratio of 0.830, while the cracks which developed as corner cracks had an average ratio of 0.46. In every case, the life predictions were conservative.

4.4 TOTAL LIFE PREDICTIONS

Total life predictions were calculated by adding the initiation and propagation life predictions. Table 5 contains the total life predictions for four RCH tests. The ratio of predicted life to actual life ranged from 0.332 to 0.670. In each of the four tests the initiation life was at least 3.8 times greater than the propagation life, thus the effect of the initiation model in predicting total life is much greater than that of the propagation model for the cases considered.

For the specimens RCH8 and RCH10, the maximum notch stresses were greater than the yield strength; thus, yielding occurred at the notch root. This yielding results in compressive residual stresses which are not accounted for by the initiation model. Compressive residual stresses would lower the notch root stress after the initial yield of the first cycle. The lower notch root stresses would account for the greater than expected number of cycles to initiate the crack. For RCH11 and RCH12 the notch root stresses are at or below yielding, thus the effect of the compressive residual stresses is small. For these specimens, the life predictions were closer to the actual life then for those with the higher stresses.

TABLE 3

SUMMARY OF INITIATION PREDICTIONS

SPECIMEN ID	NOTCH STRAIN AMPLITUDE (INCH/INCH)	MEAN STRESS (KSI)	MAX. NOTCH ROOT STRESS	NOTCH STRESS AMPLITUDE (INCH/INCH)	INITIATION CRACK LENGTH (INCH)	PREDICTED CYCLES TO INITIATION	ACTUAL CYCLES TO INITIATION	N_p/N_A
RCH8	0.0041	12.9	55.6	42.77	0.023	10,700	24,694	0.433
RCH9*	0.0041	12.9	55.6	42.77	0.023	10,700	11,185	0.957
RCH10	0.0046	0.0	47.0	47.0	0.023	9,850	38,911	0.253
RCH11	0.0033	20.4	54.5	34.10	0.023	43,200	57,770	0.749
RCH12	0.0033	0.0	34.1	34.10	0.023	130,000	185,000	0.703

* Test invalid due to surface defect.

ORIGINAL PAGE IS
OF POOR QUALITY

ORIGINAL PAGE IS
OF POOR QUALITY

TABLE 4

SUMMARY OF PROPAGATION PREDICTIONS

SPECIMEN ID	INITIAL CRACK LENGTH (INCH) $a_o = \ell_m$	FINAL CRACK LENGTH (INCH) a_f	APPLIED STRESS (KSI) max	PREDICTED CYCLES N_f	ACTUAL CYCLES N_A	ACTUAL/PREDICTED CYCLES N_P/N_A
RCH1	0.023	0.125	10.67	12,600	48,600	0.26
RCH2	0.023	0.125	13.87	6,940	13,200	0.526
RCH3	0.023	0.125	26.67	960	1,280	0.75
RCH4	0.023	0.125	26.67	960	1,932	0.497
RCH5	0.023	0.125	26.67	960	1,142	0.840
RCH6	0.023	0.125	21.83	2,300	2,329	0.988
RCH7	0.023	0.125	21.33	2,300	2,335	0.985
RCH8	0.023	0.125	26.67	960	1,895	0.506
RCH9	0.023	0.125	26.67	960	3,400	0.282
RCH10	0.023	0.125	14.67	5,940	8,586	0.69
RCH11	0.023	0.125	21.33	2,300	10,105	0.228
RCH12	0.023	0.125	10.67	12,600	47,500	0.27

TABLE 5

SUMMARY OF TOTAL LIFE PREDICTIONS

SPECIMEN ID	ACTUAL INITIATION CYCLES	PREDICTED INITIATION CYCLES	ACTUAL PROPAGATION CYCLES	PREDICTED PROPAGATION CYCLES	ACTUAL TOTAL CYCLES	PREDICTED TOTAL CYCLES	TOTAL PREDICTED CYCLES / TOTAL ACTUAL CYCLES
RCH8	24,694	10,700	1,895	960	26,589	11,660	0.439
RCH10	38,911	9,850	8,586	5,940	47,497	15,790	0.332
RCH11	57,770	43,200	10,105	2,300	67,875	45,500	0.670
RCH12	185,000	130,000	47,500	12,600	232,500	142,600	0.613

ORIGINAL PAGE IS
OF POOR QUALITY

SECTION 5

SUMMARY OF WORK ACCOMPLISHED AND WORK PLANNED FOR NEXT PERIOD

Between 1 September 1982 and 31 March 1983, the following work was accomplished.

A. Baseline testing of 2024-T3 Aluminum was conducted.

B. Life predictions using crack initiation and crack propagation models were made.

C. Fatigue tests were conducted on the 2024-T3 Aluminum.

D. The initiation and propagation models were evaluated.

Between 1 April and 31 September 1983, the following work will be accomplished.

A. Strain life tests will be continued for the 2024-T3 Aluminum.

B. The effect of residual stresses on crack initiation and propagation will be examined.

C. The initiation and propagation models will be modified to incorporate the residual stress effects.

D. Empirical mean stress models will be developed based on the strain life data generated. These models will be used to improve initiation life predictions.

REFERENCES

1. Dowling, N. E., "Fatigue at Notches and the Local Strain and Fracture Mechanics Approaches," Fracture Mechanics, ASTM STP 677, C. W. Smith, Ed., American Society for Testing and Materials, 1979, pp. 247-273.

2. Leis, B. N. and Forte, T. P., "Fatigue Growth of Initially Physically Short Cracks in Notched Aluminum and Steel Plates," Fracture Mechanics: Thirteenth Conference, ASTM STP 743, Richards Roberts, Ed., American Society for Testing and Materials, 1981, pp. 100-122.

3. El Haddad, M. H., Smith K. N., and Topper, T. H., "A Strain Based Intensity Factor Solution for Short Fatigue Cracks Initiating from Notches," Fracture Mechanics, ASTM STP 677, C. W. Smith Eds., American Society for Testing and Materials, 1979, pp. 274-289.

4. Landgraf, R. W., Mitchell, M. R., LaPointe, N. R., "Monotonic and Cyclic Properties of Engineering Materials," Scientific Research Staff Report, Ford Motor Company.

5. Sandor, Bela I., "Fundamentals of Stress and Strain," The University of Wisconsin Press, Ltd., 1972.

6. Wygonik, R. H., "Compilation of Fracture Mechanics Data," Aluminum Company of America, Alcoa Research Laboratories, New Kensington, Pa., Subcontract on Contract No. F33615-73-C-5015 (June 12, 1973).

7. J. S. Newman, Jr. and I. S. Raju, "Stress-Intensity Factor Equations for Cracks in Three-Dimensional Finite Bodies," NASA TM83200, NASA Langley Research Center, August 1981.

8. Gallagher, J. P., F. J. Giessler, A. P. Berens and R. M. Engle, Jr., "USAF Damage Tolerant Design Handbook: Guidelines for the Analysis and Design of Damage Tolerant Aircraft Structures," AFWAL-TR-82-3073, October 1982.

9. Dubensky, Robert G., "Fatigue Crack Propagation in 2024-T3 and 7075-T6 Aluminum Alloys at High Stresses," NASA CR-1732, March 1971.